Structural characterization of the epitaxially grown core-shell ZnTe/ZnMgTe nanowires

E. Dynowska[a*], J. Z. Domagała[a], P. Romanowski[a], S. Kret[a],
E. Janik[a], P.Wojnar[a] and W. Caliebe[b]

[a]*Institute of Physics, Polish Academy of Sciences, al. Lotników 32/46, PL-02668 Warszawa, Poland*
[b]*HASYLAB at DESY, Notkestr. 85, D-22603 Hamburg, Germany*

Keywords: synchrotron radiation, X-ray diffraction, nanowires, MBE, II-VI compounds,

*e-mail: dynow@ifpan.edu.pl

Abstract

We report the method of the epitaxial growth of the core-shell ZnTe/ZnMgTe nanowires. The morphology and the crystal structure of several samples grown in different processes have been studied by scanning electron microscopy, high resolution transmission electron microscopy and X-ray diffraction methods. It was shown that the ZnMgTe shell growth was clearly epitaxial with a good crystal quality. The average lattice spacing of the ZnTe cores and ZnMgTe shells have been calculated and Mg content in the shells has been estimated. It was documented that growing the shell lattice mismatched to the core induces the strain in the core. The model of the strain creation mechanism has been proposed. The presence of a shell with a larger energy gap than that of the core results in a strong emission in the spectral region near the band edge.

1. Introduction

Semiconductor nanowires (NWs) can be used to build effective nanosensors and photovoltaic devices due to their extremely large surface-to-volume ratio. On the other hand, the surface defects, especially surface states, significantly reduce the carrier lifetime affecting the electron transport and optical properties. This causes, for example, a decrease of the near band edge emission (Janik et al., 2006, Skold et.al.,2005, Zaleszczyk et al., 2008). Therefore, a surface passivation is of great importance, especially for ZnTe NWs which oxidize easily. To improve the physical properties of semiconductor nanostructures a lot of effort has been devoted to find a prper preparation manner of a core-shell composite semiconductor structure by combining different materials (Chao et al., 2010, Radovanovic et al., Skold et.al.,2005, 2005, Xie et al., 2005). It was shown that a surface passivation can be achieved by forming a

shell of a large band gap material around the NW core so the surface states are moved away from the charge carriers confined in the core. In the case of ZnTe NWs the influence of surface effects on the electrical and optical properties can be reduced by forming the ZnMgTe shell around the ZnTe core. The presence of the ZnMgTe shell, a semiconductor with a larger energy gap, than that of the core results in the appearance of a strong emission near the core band edge (Wojnar et al., 2011).

In this paper we describe on the method of growth and the results of structural characterization of the core-shell ZnTe/$Zn_{1-x}Mg_xTe$ NWs grown on the GaAs(111) substrate.

2. Experimental details

The ZnTe NWs were grown by molecular beem epitaxy (MBE) by employing the vapour-liquid-solid growth mechanism assisted by gold catalysts at the temperature of about 400ºC. The growth procedure of ZnTe NWs was described in detail previously (Janik et al., 2007). The $Zn_{1-x}Mg_xTe$ shells were produced immediately after the growth of the ~1.5 μm long ZnTe cores. In order to produce the shells the substrate temperature was reduced to the value 250 - 300 ºC which stops the axial growth of NWs and forces the radial growth of $Zn_{1-x}Mg_xTe$ shell. The post-growth annealing has been applied for three selected samples. The technological parameters concerning the core and the shell growth temperatures as well as the time of a shell growth for all studied samples are listed in the Table 1. Moreover, the samples differed with respect to the composition of their shells: the samples described by symbols 022411 A, B and C had significantly higher content of magnesium than others samples stored in the table.

The morphology and structure of the core-shell NWs were studied by the field-emission scanning electron microscopy (FE-SEM Leo 540), the high resolution transmission electron microscopy (HRTEM) using FEI TITAN Cube 80-300 microscope operating at 300kV and X-ray diffraction (XRD) methods with the use of synchrotron radiation as well as the laboratory X-ray source. The aberration corrected HRTEM (CS-HRTEM), high-angle annular dark field (HAADF-STEM) and energy dispersive spectroscopy (ED) were used for studies of the NWs deposited on the holey carbon films supported by Cu mesh.

The X-ray diffraction measurements performed with the use of synchrotron radiation were done at the W1 beamline at DESY-HASYLAB in Hamburg. The monochromatic X-ray beam of the wavelength λ = 1.54056 Å was used. Two modes of measurement were applied: symmetrical 2θ-ω scan and coplanar 2θ scan in the glancing incidence geometry. In the first mode of measurement the detector position (2θ angle) is coupled with the maximum intensity of the relevant rocking curve (ω angle) resulting from the crystallographic orientation of GaAs substrate. Such measurement allows to detect the lattice planes parallel to the crystallographic orientation of the substrate. In the second mode of measurement the rotation axis of the sample (ω axis) has been aligned exactly with the sample surface and then the sample was rotated about this axis by a very small angle α (here equal to 1°). The angular position of the sample with respect to the incident X-ray beam (α) was fixed during measurement while the detector was rotated in the wide range of 2θ angles in the plane perpendicular to the sample surface. Such technique is very sensitive and can be applied to very thin layers because the layer volume irradiated by X-ray beam under so small angle is much larger than that in the case of a classical 2θ-θ scan. Some samples were measured using multipurpose X'Pert PRO MPD diffractometer (Bragg–Brentano diffraction geometry) equipped with a strip detector and an incident-beam Johansson monochromator. The Cu $K_{\alpha 1}$ radiation of the wavelength λ = 1.54056 Å was applied.

3. Results and discussion

The seven samples of core-shell ZnTe/$Zn_{1-x}Mg_xTe$ NWs grown on the (111)-oriented GaAs substrate were the object of present studies. The results of present measurements confirmed earlier results concerning the ZnTe NWs, namely, that the growth axis of the NWs is of <111> type. The NWs grew along <111> direction of the GaAs substrate, independently on the given substrate orientation (Janik et al., 2007). If the NWs are grown on (111) oriented substrate (our case) they are either perpendicular to the (111) lattice plane of the substrate or form an angle of 19.5° with this plane. The majority of NWs seen in the FE-SEM image shown in Fig. 1 are perpendicular to the GaAs surface and only these NWs can be characterized by X-ray diffraction. The X-ray diffraction patterns performed for the samples in the symmetrical geometry (2θ-ω scan) also confirmed the epitaxial relation between the substrate and the NWs. As an example the 2θ-ω scan in the large range of 2θ angles performed on the sample 090110A is shown in the Fig.2a. The three orders of reflections

related to the (111) lattice planes of GaAs substrate and of the NWs are visible in the pattern presented in this figure. The X-ray measurement performed in the glancing incidence mode (2θ scan), presented in Fig. 2b, shows the polycrystalline pattern which indicates on a presence thin polycrystalline layer grown on the GaAs substrate between NWs. The analysis of this pattern allows to indentify reflections from ZnTe and ZnMgTe phases, respectively. The X-ray diffraction patterns shown in Fig. 2a,b are typical for all studied samples.

A zoom of the symmetrical patterns in the vicinity of 333 NWs peaks allows to notice their splitting: the right side peak originates from the ZnTe core while the left side one is related to the ZnMgTe shell (Fig. 3 and Fig. 4). This splitting indicates the epitaxial character of the $Zn_{1-x}Mg_xTe$ shell growth and demonstrates that the shell has the same crystallographic orientation as that of the ZnTe core. The distance between these two peaks depends obviously on the Mg content in the shell – for the sample with higher Mg content the splitting is larger (Fig. 4).

An epitaxial relation between the shell and core in the samples under investigation has been also confirmed by the HRTEM studies. The HRTEM images presented in the Fig. 5 show quite abrupt increase of the brightness on the NWs border. Such average intensity modification can be related rather to the presence of the lighter element Mg in the shell than that corresponding to the NWs border thickness drop effect. The Z-contrast, imaging generated by HAADF-STEM (not shown) confirmed that material of the shell has lower average atomic number. Finally, the EDS measurements clearly detect higher Mg to Zn signal ratio on the border of the NWs. From HRTEM images we determined the shell thickness ranging from 8 to 12 nm. The interface between the core and shell is abrupt and its width is not larger than 1 or 2 lattice spacings. It is also clear that the stacking faults (SF) present in the core propagate into the ZnMgTe shell. The surface of the NWs is covered by about 4 nm thick polycrystalline layer which cannot be detected by X-ray diffraction due to very small sizes of forming it nanocrystalites .

The X-ray results for the first group of samples, presented in the Fig. 3, indicate a low content of Mg in the shells – the splitting of the peaks is small, but noticeable. Fig. 3*a*,*b* present the part of X-ray pattern in the vicinity of the 333 NWs peaks of the samples 090110A and 090110B which differed by the time of the shell growth which was longer for the sample 090110B. In consequence, the intensity of the left side peak on the pattern shown in the Fig.3*b* is higher than that presented in the Fig.3*a*. The Fig. 3*c* and 3*d* show the influence of the post-growth annealing on the structure of NWs. In the non annealed sample, 092910B,

the splitting of the 333 NWs peak is clearly visible (Fig. 3*c*), while in annealed sample, 092910A, only small asymmetry on the left side of the peak can be noticed (Fig. 3*d*). It is probably caused by the partial diffusion of Mg atoms to the core during annealing procedure.

The results obtained for the second group of samples are presented in the Fig. 4*a*, *b* and *c*. Intentionally the shells in these NWs contained significantly more Mg than the previous samples, therefore the distances between components of splitted peaks are larger (Fig.4). The shell of the sample 022411B has been grown at lower temperature than that of the sample 022411A – according to the results presented in the Fig. 4*a* and Fig.4*b* the more pronounced splitting of the NWs peaks is observed for the sample with lower temperature of the shell growth.

On the base of X-ray measurements described above the lattice parameters of the shell and core were calculated from the angle positions of the splitted 333 NWs peaks. The obtained results were corrected with respect to the 333 peak from GaAs substrate. The chemical compositions x of the $Zn_{1-x}Mg_xTe$ shells were estimated from the lattice parameters values according to the Vegard's rule, respectively. The obtained results are collected in the Table 2.

It should be noticed that the lattice parameter of the ZnTe core of different samples (a = 0.6114 - 0.6120 nm) is larger not only than that of bulk ZnTe (a = 0.6103 nm, according to JCPDS, 15-0746), but also than the lattice parameter of the uncovered ZnTe NWs grown on (111) substrate: a = 0.6110 nm. The last value was determined and justified in the earlier paper (Dynowska et al., 2009). We believe that source of the increase of the lattice parameter of covered ZnTe NWs is the tensile strain of ZnTe core caused by $Zn_{1-x}Mg_xTe$ shell. The model showing possible mechanism of such strain creation is presented in Fig. 6. As it is known, the epitaxial growth of lattice mismatched material generates the strain and/or relaxation processes. Generally, the lattice spacing in ZnMgTe are larger than those in ZnTe – exactly the lattice mismatch between core and shell in our samples are f_1 = 0.004 and f_2 = 0.01, respectively. During the shell growth the relaxation process causes decrease of the (111) lattice spacing of ZnMgTe shell with simultaneous increase of the (111) lattice spacing of ZnTe core. Taking into account all X-ray results we can conclude that ZnMgTe shell growth is epitaxial but not pseudomorphic. The generation of a strain in the core was also observed for the $GaAs/Ga_xIn_{1-x}P$ NWs (Skold et.al., 2005) where the strain effects were monitored by the band gap changes of the core.

4. Conclusions

The XRD and HRTEM studies confirmed the epitaxial character of the shells in all studied samples. The HRTEM images of the single NW showed directly the epitaxial character of the shell and the X-ray patterns confirmed this by observation of the splitting of core-shell NWs peaks. On the base of X-ray measurements the average lattice spacing of the ZnTe core and ZnMgTe shells have been calculated. In consequence, the presence of strain induced in the ZnTe core by the lattice mismatched shell has been documented as well as the Mg content in the shells could be estimated. The mechanism of the strain creation in the NW core has been proposed and schematically shown in Fig. 6.

Let us notice that the electron microscopy studies give the information from very small part of the investigated material – in contrary to the X-ray measurements which give an averaged information from relatively large volume of the sample. It is particularly important in the case of NWs: using the microscopy methods we can see detailed structure of the individual NW, but we cannot be sure whether all, or at least the majority of the NWs have similar structure. We can prove it by the X-ray methods. The averaging process during the X-ray measurements takes place in two steps: within each NW and on the set of a large number of NWs. Then, observation of the splitting of core-shell NWs peaks for all samples in X-ray diffraction measurements confirm the result of TEM studies.

The results of structural characterization have been obtained for the seven samples of the core-shell ZnTe/ZnMgTe NWs. The samples were grown according to the special procedure elaborated in order to find the best technological conditions for forming an epitaxial radial shell around the nanowires. The influence of different technological parameters on the structure of the NWs was determined by our studies. It should be underlined that earlier attempts of growing different shells around the ZnTe core lead to the nanocrystalline character of them, for example: (Gas et al., 2011, Janik et al., 2010).

Concluding, the use of the combined methods of characterization allowed the deeper understanding of the structural properties of investigated core-shell NWs.

Acknowledgements

The research has been supported by the European Union within European Regional Development Fund through Innovative Economy grant (POIG.01.02-00-008/08) and European Community-Research Infrastructure Action under the FP6 "Structuring the European Research Area" Programme (through the Integrated Infrastructure Initiative "Integrating Activity on Synchrotron and Free Electron Laser Science", Contract RII3-CT-2004-506008). TEM investigation was supported by European Regional Development Fund within the Innovative Economy Operational Programme 2007-2013 “Analytical high resolution transmission electron microscope for nanoscience, nanotechnology and spintronics” No POIG.02.01-00-14-032/08.

References

Chao, H.Y., Cheng, J.H., Lu, J.Y., Chang, Y.H., Cheng, C.L., Chen, Y.F., 2010. Growth and characterization of type-II ZnO/ZnTe core-shell nanowire arrays for solar cell applications. Superlattices and Microstructures 47, 160–164.

Dynowska, E., Szuszkiewicz, W., Domagala, J.Z., Janik, E., Presz, A., Wojtowicz, T., Karczewski, G., 2009. X-ray characterization of catalytically grown ZnTe and ZnMgTe nanowires. Radiat. Phys. Chem. 78, S120–S124.

Gas, K., Janik, E., Zaleszczyk, W., Dynowska, E., Kutrowski, M., Kamińska, A., Morhange, J.F., Wachnicki, Ł., Wojciechowski, T., Hołyst, R., Godlewski, M., Guziewicz, E., Wojtowicz, W., Szuszkiewicz, W., 2011. Selected optical properties of core/shell ZnMnTe/ZnO nanowire structures,. Phys. Status Solidi B **248**, 1592

Janik, E., Dluzewski, P., Kret, S., Presz, A., Kirmse, H., Neumann, W., Zaleszczyk, W., Baczewski, L.T., Petroutchik, A., Dynowska, E., Sadowski, J., Caliebe, W., Karczewski, G., Wojtowicz, T., 2007. Catalytic growth of ZnTe nanowires by molecular beam epitaxy: structural studies. Nanotechnology 18, 475606-1–475606-8.

Janik, E., Sadowski, J., Dluzewski, P., Kret, S., Baczewski, L.T., Petroutchik, A., Lusakowska, E., Wrobel, J., Zaleszczyk, W., Karczewski, G., Wojtowicz, T., Presz, A., 2006. ZnTe nanowires grown on GaAs(100) substrates by molecular beam epitaxy. Appl. Phys. Lett. 89, 133114-1–133114-3.

Radovanovic, P.V., Barrelet, C.J., Gradecak, S., Qiang, F., Lieber, C.M., 2005. . General synthesis of manganese-doped II-VI and III-V semiconductor nanowires. Nano Lett. 5, 1407–1411.

Skold, N., Karlsson, L.S., Larsson, M.W., Pistol, M., Seifert, W., Tragargh, J., Samuelson, L., 2005. Growth and optical properties of strained GaAs-$Ga_xIn_{1-x}P$ core-shell nanowires. Nano Lett. 5, 1943–1947.

Wojnar, P., Janik, E., Kret, S., Dynowska, E., Baczewski, L.T., Karczewski, G., Wojtowicz, T., 2011. Near band edge emission of Te-based nanowire heterostructures, Proceedings of the 15th International Conference on II-VI Compounds, 34.

Xie, R., Zhong, X., Basche, T., 2005. Synthesis, characterization, and spectroscopy of type-II core/shell semiconductor nanocrystals with ZnTe cores. Adv. Mater. 17, 2741–2745.

Zaleszczyk, W., Janik, E., Presz, A., Dluzewski, P., Kret, S., Szuszkiewicz, W., Morhange, J.F., Dynowska, E., Kirmse, H., Neumann, W., Petroutchik, A., Baczewski, L.T., Karczewski, G., Wojtowicz, T., 2008. $Zn_{1-x}Mn_xTe$ diluted magnetic semiconductor nanowires grown by molecular beam epitaxy. Nano Lett. 8, 4061–4065.

Table 1

The technological parameters of the growth process of core-shell ZnTe/ZnMgTe NWs. T_{axial} and T_{radial} denote the growth temperature of the ZnTe core and ZnMgTe shell, respectively.

Sample	T_{axial} ZnTe core (relative) (°C)	T_{radial} $Zn_{1-x}Mg_xTe$ shell (relative) (°C)	Time of the shell growth (min)	Post growth annealing	
				Temperature (°C)	Time (min)
090110A	400	250-300	10	450	30
090110B	400	250-300	15	450	30
092910A	400	250-300	10	450	30
092910B	400	250-300	10	none	none
022411A	400	250-300	10	none	none
022411B	400	220-270	10	none	none
022411C	400	250-300	15	none	none

Table 2

The lattice parameters of the ZnTe core and ZnMgTe shell calculated in the [111] crystallographic direction and the estimated Mg content for studied samples.

Sample	Lattice parameter of the ZnTe core a (nm) ± 0.0002	Lattice parameter of the $Zn_{1-x}Mg_xTe$ shell a (nm) ± 0.0002	Mg content x ± 0.01
090110A	0.6115	0.6139	0.11
090110B	0.6120	0.6137	0.12
092910A	-	-	-
092910B	0.6114	0.6141	0.11
022411A	0.6118	0.6193	0.28
022411B	0.6119	0.6189	0.27
022411C	0.6117	0.6186	0.26

Fig. 1

FE-SEM side-view image of the ZnTe/ZnMgTe core-shell NWs of the sample 090110A

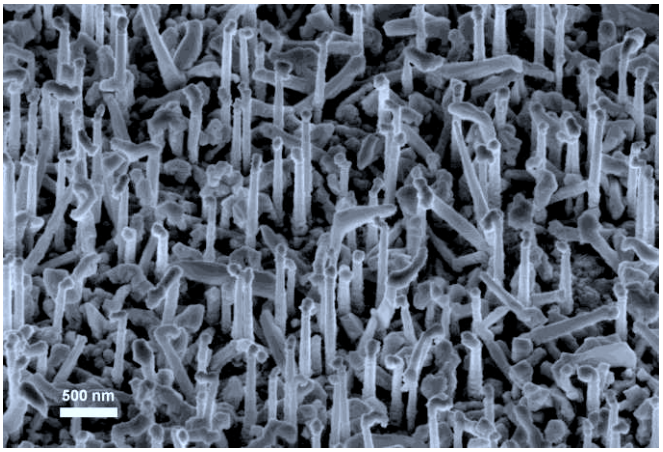

Fig. 2

The diffraction patterns of the 090110 A sample performed with the use of synchrotron radiation: (a) – symmetrical 2θ-ω scan; (b) - 2θ scan in glancing incidence geometry.

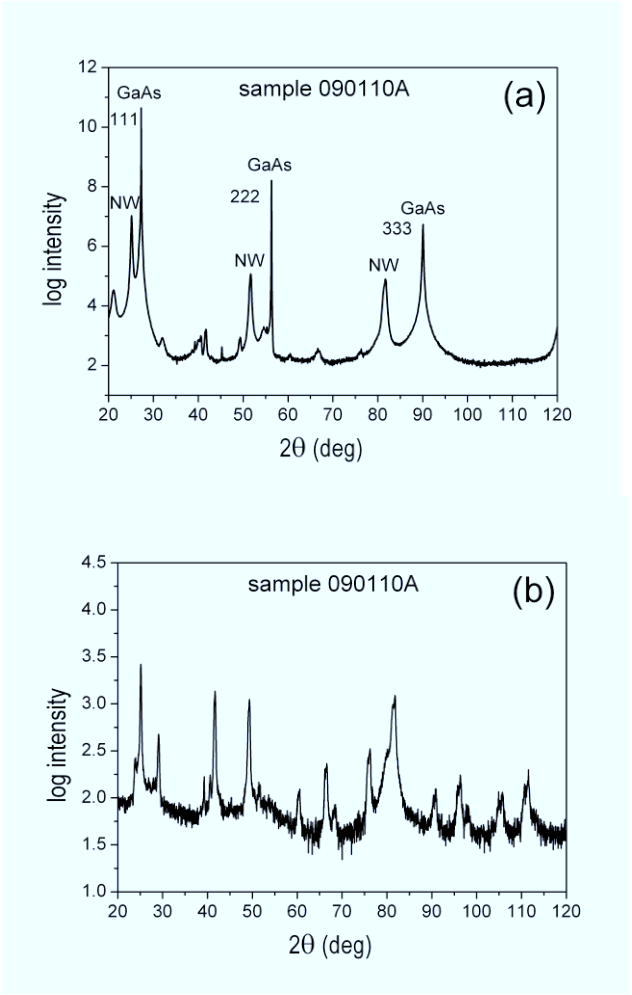

Fig. 3

The part of the 2θ-ω patterns in the vicinity of the 333 NWs peaks of the samples: (a) –10 minutes of the shell growth, (b) – 15 minutes of the shell growth, (c) – not annealed sample, (d) – annealed sample

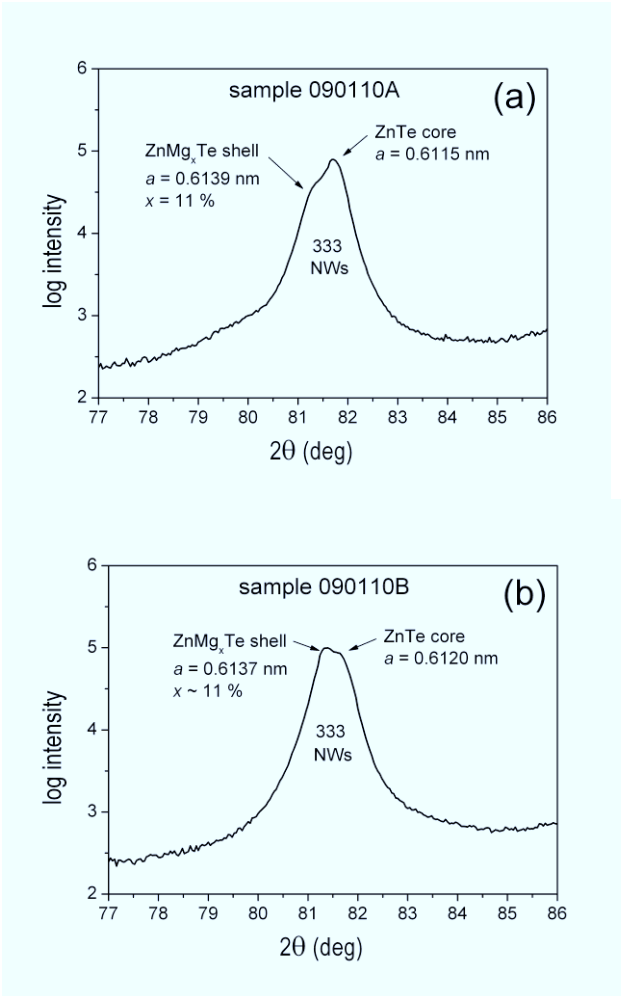

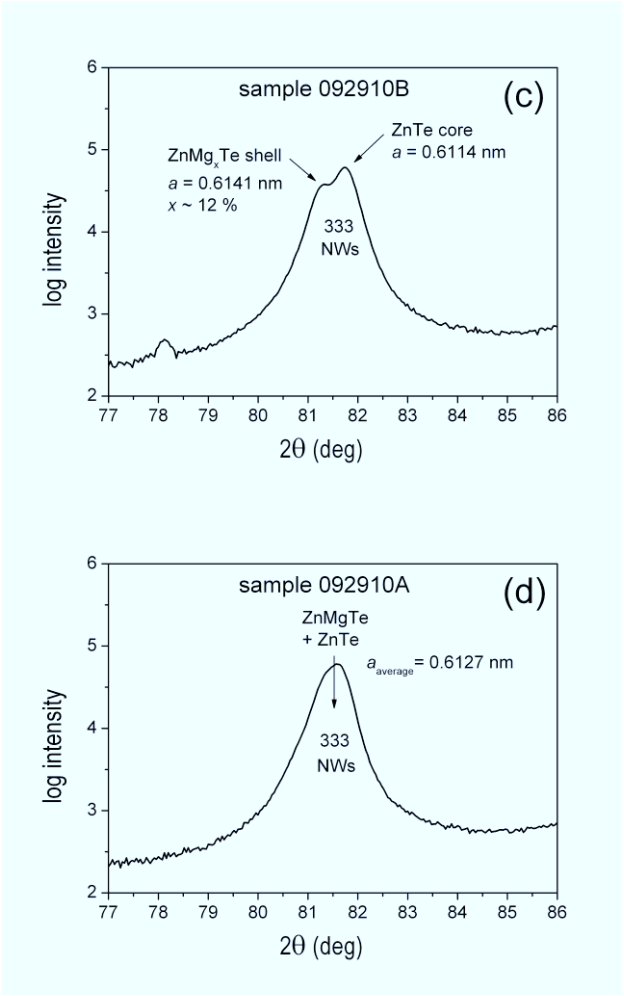
sample 092910B
(c)
ZnTe core
a = 0.6114 nm
ZnMgxTe shell
a = 0.6141 nm
x ~ 12 %
333
NWs
log intensity
2θ (deg)
sample 092910A
(d)
ZnMgTe
+ ZnTe
a average = 0.6127 nm
333
NWs
log intensity
2θ (deg)

Fig. 4

The part of 2θ-ω patterns (X'Pert diffractometer) in the vicinity of the 333 NWs peaks of the samples: (a) – temperature of the shell growth ~250-300 ºC; (b) – temperature of the shell growth ~220-270 ºC (time of the shell growth was 10 minutes in both samples); (c) – time of the shell growth was 15 minutes, temperature ~250-300 ºC.

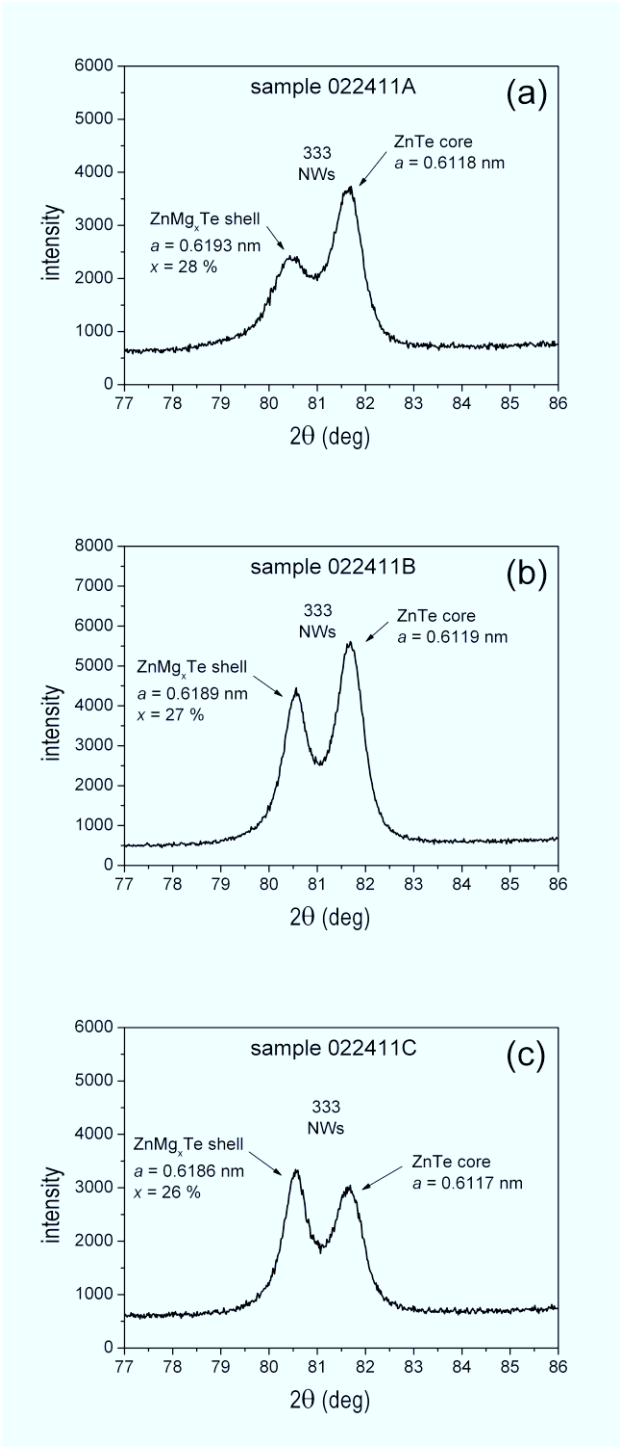

Fig. 5

The HRTEM images of (a) – <110> zone axis of the individual core-shell ZnMgTe NW deposited on a holey carbon film, (b) – enlarger part of the border of the NW shown in the figure (a). The brighter part clearly visible in the image (b) is related to the shell. The lattice planes of the shell have exactly the same orientation as those in the core which confirms the epitaxial character of the shell. We can observe that the SFs existing inside the core propagate to the shell.

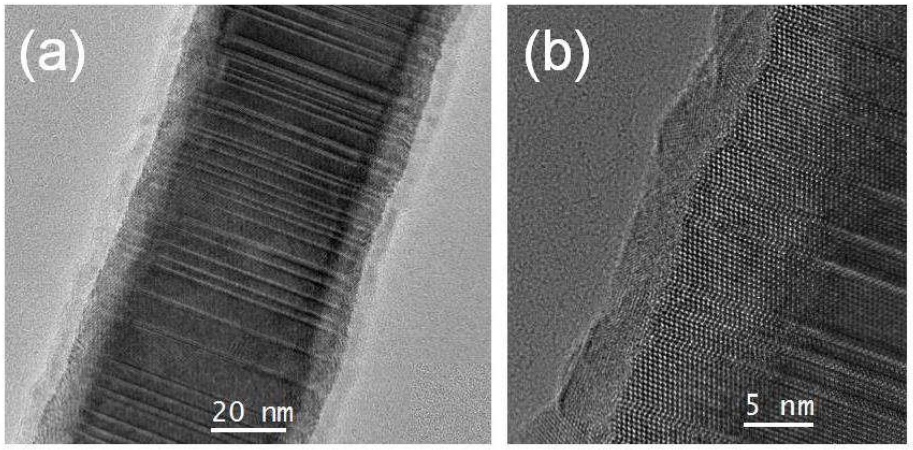

Fig. 6

Schematic illustration of the strain induced in the core by the lattice mismatched shell: (a) – top view and (b) – side view of the core-shell NW.